Process parameter optimization of Laser Micrometallurgy of AZ31 alloy

ANDRZEJ PAWLAK*, EDWARD CHLEBUS*

*Centre for Advanced Manufacturing Technologies, Wroclaw University of Technology, andrzej.p.pawlak@pwr.edu.pl

Abstract: *This paper presents process optimization results of laser powder micrometallurgy of AZ31 alloy, for eliminating porosity in melted material. Full factorial design of three factors at three levels was conducted, and the influence of laser beam power, point distance and exposure time was examined.*

Keywords: *SLM, magnesium alloy, Design of Experiments, porosity*

1. Introduction

Additive manufacturing Technologies – Rapid Prototyping gain more market shares, thanks to the wider freedom of forming possible geometries than with conventional manufacturing techniques. This leads to intensive development of these technologies and new materials [1].

Magnesium is one of the lightest construction materials used in the industry, with very high specific strength values (100-110 km) [2]. Despite of numerous occurrence on Earth, due to difficulties in processing and high reactivity in air atmosphere it is not widely used.

Combination of additive manufacturing technologies, which allow manufacture of lightweight spatial structures, with application of lightweight metal alloys, could yield with demanded results nowadays, when emphasis is placed on strength to mass ratio. First interests in the presented issue have been reported by research institutes [3-6].

Laser Micrometallurgy technology (LMM) is one of the additive manufacturing technologies, that allows to manufacture layer-by-layer objects from metal alloy powders, characterized by almost 100% dense material which has been melted. The Melting process in LMM technology is realized by a high power focused laser beam, which melts consecutive layers of newly deposited powder (by a wiper) according to sequential cross-sections of the manufactured objects [7].

2. Material and Methods

Full factorial experiment was designed with three factors at three levels. The changed LMM process parameters were: laser power, point distance between scanning points, and exposure time of laser spot in consecutive points. Values of analyzed parameters are shown in Tab. 1.

Based on selected values, 27 specimens with different parameter sets were planned. They were manufactured, using a ReaLizer SLM50 device, which allows melting of metal alloy powders layer-by-layer with a fibrous laser (max power 100 W), focused to a 100 μm diameter. Cuboid specimens of 5x3x3 mm, were manufactured with layer thickness of 50 μm and 100 μm line spacing. Spherical powder of AZ31, magnesium alloy, was used with particle size of 45-100 μm (TLS Technik GmbH & Co Spezialpulver KG).

Tab. 1. Defined values of analyzed process parameters at each level

Factors	Levels			
	codes	-1	0	1
Laser Power (P) [W]	x_1	60	75	90
point distance ($pt_{distance}$) [μm]	x_2	10	15	20
exposure time ($t_{exposure}$) [μs]	x_3	40	80	120

Three repetitions of presented experimental design were performed. Manufactured specimens were mounted in two-component resin in order to prepare a metallographic sections. Obtained cross-sections were photographed with a confocal microscope (Fig. 1). Pictures in greyscale were converted to monochromatic, and analysis of counting white and black pixels was realized, which indicates base material and pores respectively. Ratio of black pixels to total amount of pixels in analysed cross-section area defines porosity. Results were collected and analyzed in software Minitab 17.

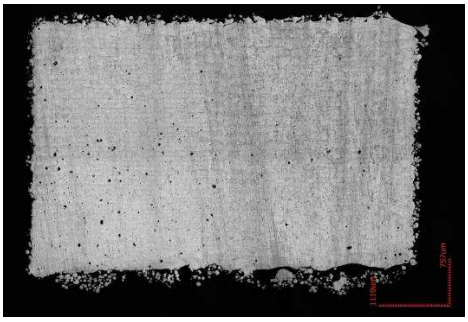

Fig. 1. Example picture of specimen cross-section (Specimen no. 25)

3. Design of Experiments

In most research papers, the basic parameter which describes the LMM process is line energy density, next to scan velocity (V_{scan}) (Fig. 2). Line energy density is a quotient of laser power (P) over the product of scan velocity and spot size diameter (*spot size*) (Eq. 1) [8-9]. Based on mentioned coefficient, relationship between used process parameter values and obtained density of melted material and mechanical properties are given.

$$Line\ energy\ density = \frac{P}{v_{scan} * spotsize}\ [J*mm^{-2}] \quad (1)$$

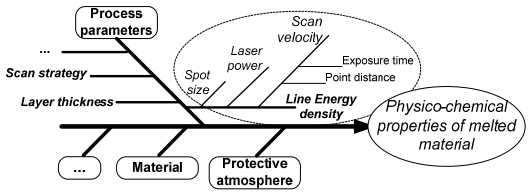

Fig. 2. Ishikava diagram of factors influencing on SLM process.

Scan velocity also is not defined directly, but it is realized discretely point after point, separated by defined point distance ($pt_{distance}$), with stops at each point for set time in parameter time exposure ($t_{exposure}$) – eq. 2

$$V_{scan} = \frac{pt_{distance}}{t_{exposure}}\ [mm*s^{-1}] \quad (2)$$

In order to perform the optimization, a Design of Experiments approach was used. Due to the process characteristics, occurring relations are not linear. That's why the factorial designs at two factor level, did not result in a proper mathematical model. Despite that fact, such plans have been commonly used, due to small amount of experiments to be performed (2^k, where k is the number of analysed factors). Mathematical model obtained as a result of such a experiments, did not allow to present square polynomial relations for more than one factor, because the square term is not differentiated from the absolute term.

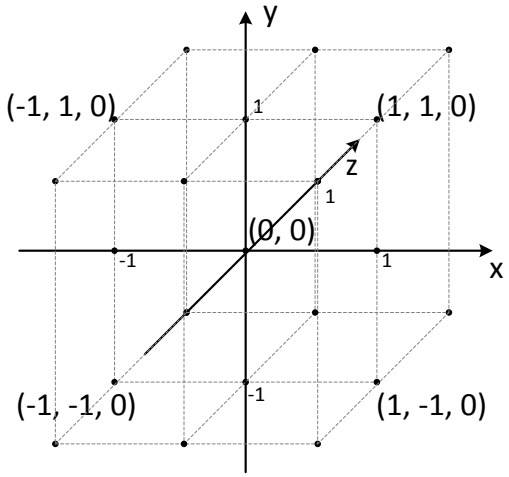

Fig. 3. Scheme of full factorial experiment design for three factors at three levels.

General experimental plan, which could be performed to determine significance of analyzed factors is full factorial experiment at three levels (3^k). In case of three analyzed factors, the design will require 27 experiments, compared to 8 in a two level factorial design (Fig. 3). It is possible to determine an equation of a function, which includes interactions between linear and square elements. The general equation is given in the form:

$$\begin{aligned} f(x) &= \alpha_0 + \alpha_1 x_1 + \alpha_2 x_2 + \alpha_3 x_3 + \alpha_{12} x_1 x_2 \\ &+ \alpha_{13} x_1 x_3 + \alpha_{23} x_2 x_3 + \alpha_{123} x_1 x_2 x_3 + \alpha_{11} x_1^2 \\ &+ \alpha_{22} x_2^2 + \alpha_{33} x_3^2 + \alpha_{22} x_2^2 + \alpha_{33} x_3^2 \\ &+ \alpha_{122} x_1 x_2^2 + \alpha_{133} x_1 x_3^2 + \alpha_{211} x_2 x_1^2 \\ &+ \alpha_{233} x_2 x_3^2 + \alpha_{311} x_3 x_1^2 + \alpha_{322} x_3 x_2^2 \\ &+ \alpha_{12233} x_1 x_2^2 x_3^2 + \alpha_{21133} x_2 x_1^2 x_3^2 \\ &+ \alpha_{31122} x_3 x_1^2 x_2^2 + \alpha_{1122} x_1^2 x_2^2 + \alpha_{1133} x_1^2 x_3^2 \\ &+ \alpha_{2233} x_2^2 x_3^2 + \alpha_{112233} x_1^2 x_2^2 x_3^2 + \alpha_{1233} x_1 x_2 x_3^2 \\ &+ \alpha_{1322} x_1 x_3 x_2^2 + \alpha_{2311} x_2 x_3 x_1^2, \end{aligned} \quad (3)$$

where $f(x)$ is an expected value, and α are unknown elements of square regression.

In this work process optimization was performed, using three factors. Chosen factors allow to define porosity in dependence of the used line energy density – laser power, point distance and exposure time. The spot size parameter is dependent on the

installed focusing lens and remains at a fixed value during the research. Minitab and Design of Experiments approach was used to specify the involvement of the analyzed factors.

4. Results and Discussion

Process parameters used in the experiments, obtained average porosity and standard deviation are presented in Table A. It can be observed, that an increase of laser power leads to a decrease of porosity in the material. At the highest laser power, about 1% of porosity was reached. On the other hand, when analyzing values of the line energy density it should be noticed that also the scan velocity has strong influences on porosity – maximum densities were obtained at the lowest line energy density values.

Statistical analysis of variance (ANOVA) was calculated in Minitab 17. Table B shows that the most influential factor on porosity was laser power and point distance, which determines scan velocity. It is proven by specified interaction between these parameters.

Main effects plot of factorial analysis, proves that the largest changes in porosity 3% change, is caused by a 50% laser power change from 60 to 90 W (Fig. 4). Exposure time at each scanning point, has an opposite effect to other analyzed parameters – increasing values of $t_{exposure}$ increases porosity in the material. Extended exposure of a point, could lead to local overheating of the material and even to evaporation and pores formation.

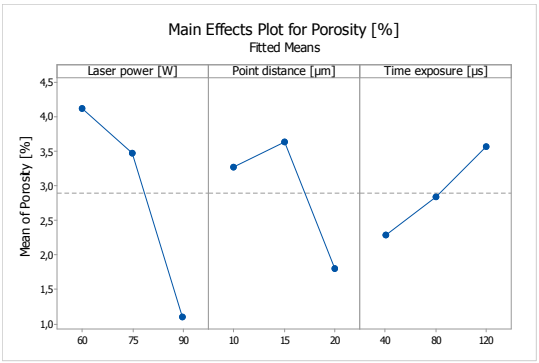

Fig. 4. Main effects plot of analyzed factors in performer experiment

The plot of interactions between analyzed factors is shown at Fig. 5. The clearest interaction exhibits between laser power and point distance for lower powers. Interaction between point distance and exposure time is more legible at 10 and 15 µm distance.

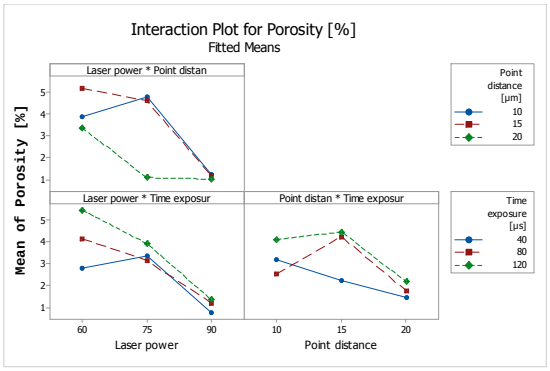

Fig. 5. Plot of reciprocal involvement for analyzed factors

Analyzing of the plot of porosity vs. energy density of various laser power, it could be observed that for the highest laser power (90W), linear relation occurs (Fig. 6). For lower laser power values this relation is not present. High values of linear energy density, resulting in increase of porosity in material, induces probability of material evaporation, because of too high intensity of laser radiation.

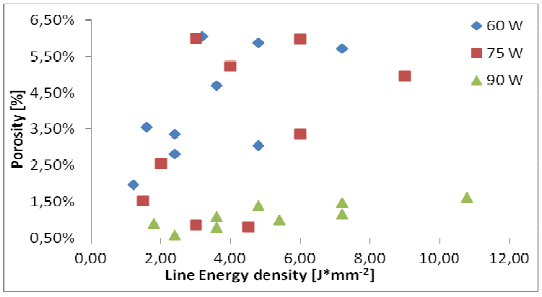

Fig. 6. Relation between gained porosity values and used line energy density

5. Conclusions

As a result of the performed experiments, specimens of melted magnesium alloy powder were obtained with repeatable porosity below 1%. The lowest porosity was reached using the highest analyzed laser power, which also had the highest influence on the obtained results. A slightly smaller influence on the porosity had changes of the point distance. Essential is also interaction between mentioned factors. Increase of laser power leads to increase of line energy density values, but the scan velocity also has a crucial impact, because of the relevance of the distance between points. That is why it is imprecise to present material porosity values relative to line energy density, without remarks on constituent factors on this value.

As a result of conducted research, an analytical mathematical model was defined, which describes relation between porosity in material and used in experimental analysis process parameters (eq. 4)

$$
\begin{aligned}
f(x) &= -1650 + 47{,}83x_1 + 204{,}5x_2 \\
&+ 33{,}06x_3 - 5{,}932x_1x_2 - 0{,}9977x_1x_3 \\
&- 4{,}206x_2x_3 + 0{,}1278x_1x_2x_3 - 0{,}3262x_1^2 \\
&- 6{,}238x_2^2 - 0{,}1324x_3^2 + 0{,}1809x_1x_2^2 \\
&+ 0{,}0042x_1x_3^2 + 0{,}0405x_2x_1^2 + 0{,}0161x_2x_3^2 \\
&+ 0{,}007x_3x_1^2 + 0{,}1318x_3x_2^2 \\
&+ 0{,}00002x_1x_2^2x_3^2 + 0000004x_2x_1^2x_3^2 \\
&+ 0{,}00003x_3x_1^2x_2^2 - 0{,}0012x_1^2x_2^2 \\
&- 0{,}00003x_1^2x_3^2 - 0{,}0005x_2^2x_3^2 \\
&- 0{,}0000001x_1^2x_2^2x_3^2 - 0{,}0005x_1x_2x_3^2 \\
&- 0{,}004x_1x_3x_2^2 - 0{,}0009x_2x_3x_1^2,
\end{aligned}
\tag{4}
$$

where: x_1 – Laser power, x_2 – point distance, x_3 – exposure time.
The determination coefficient of defined relation is R=0,8423, which fits good to experimental values.

Obtained results, are the basis for further process optimization, including e.g. Layer thickness and line spacing between consecutive scan lines. During future researches, changing in scan velocity values will be realized by changes in point distance values, while short exposure time at points remains at unchanged value.

Acknowledgments

Research was co-financed by the European Union as part of the European Social Fund

References

[1] T. Wohlers. Wohlers Report. Wohlers Associates, Inc. Fort Collins. 2014.
[2] K. Oczoś, A. Kawalec, Kształtowanie metali lekkich, Wydawnictwo Naukowe PWN. Warszawa 2012. s. 49-122.
[3] C.C. Ng, M.M. Savalani, H.C. Man. Fabrication of magnesium using selective laser melting technique. Rapid Prototyping Journal 17/6: 479-490.
[4] C.C. Ng, M.M. Savalani, M.L. Lau, H.C. Man,. Microstructure and mechanical properties of selective laser melted magnesium. Applied Surface Science2011. 257: 7447-7454.
[5] B. Zhang, H. Liao, Ch. Codett. Effects of processing parameters on properties of selective laser melting Mg-9%Al powder mixture. Materials and Design2012. 34: 753-758.
[6] M.M. Savalani, C.C. Ng, H.C. Man. Selective laser melting of Magnesium for Future Applications in the Medicine. 2010 International Conference on Manufacturing Automation. 2010. s.50-54.
[6] A. Pawlak . Wpływ gęstości oddziaływania wiązki laserowej na porowatość wyrobów wytwarzanych za pomocą SLM (Selective Laser Melting), Interdyscyplinarność badań naukowych 2012, Wrocław, Oficyna Wydawnicza Politechniki Wrocławskiej, 2012. s. 335-340.
[7] K. Kempen, L. Thijs, E. Yasa, M. Badrossamay, W. Verheecke, J.P. Kruth. Process optimization and microstructural analysis for Selective Laser Melting of AlSi10Mg, 2011, Available at: http://utwired.engr.utexas.edu/lff/symposium/proceedingsArchive/pubs/Manuscripts/2011/2011-37-Kempen.pdf
[8] M. Krishnan, E. Atzeni, R. Canali, F. Calignano, D. Manfredi E.P. Ambrosio, L. Iuliano. On the effect of process parameters on properties of AlSi10Mg parts produced by DMLS. Rapid Prototyping Journal. 2014. 20(6):449-458

Appendices

Table A. Set of performed experiments, used values of parameters and obtained results

Parameter set	P	$pt_{distance}$	$t_{exposure}$	V_{scan}	Porosity [%]		Line energy density
	[W]	*[μm]*	*[μs]*	*[mm*s^{-1}]*	*mean*	*S.D.*	*[J*mm^{-2}]*
1	60	10	40	250,00	2,80	0,68	2,40
2	60	10	80	125,00	3,04	0,25	4,80
3	60	10	120	83,33	5,72	1,83	7,20
4	60	15	40	375,00	3,55	0,34	1,60
5	60	15	80	187,50	6,05	1,31	3,20
6	60	15	120	125,00	5,87	1,81	4,80
7	60	20	40	500,00	1,96	0,41	1,20
8	60	20	80	250,00	3,35	0,80	2,40
9	60	20	120	166,67	4,70	1,47	3,60
10	75	10	40	250,00	6,00	1,47	3,00
11	75	10	80	125,00	3,36	1,02	6,00
12	75	10	120	83,33	4,95	1,58	9,00
13	75	15	40	375,00	2,55	2,18	2,00
14	75	15	80	187,50	5,23	0,82	4,00
15	75	15	120	125,00	5,99	1,84	6,00
16	75	20	40	500,00	1,52	0,13	1,50
17	75	20	80	250,00	0,86	0,58	3,00
18	75	20	120	166,67	0,80	0,27	4,50
19	90	10	40	250,00	0,79	0,43	3,60
20	90	10	80	125,00	1,16	0,57	7,20
21	90	10	120	83,33	1,62	0,50	10,80
22	90	15	40	375,00	0,57	0,15	2,40
23	90	15	80	187,50	1,39	0,47	4,80
24	90	15	120	125,00	1,48	0,25	7,20
25	90	20	40	500,00	0,88	0,10	1,80
26	90	20	80	250,00	1,09	0,58	3,60
27	90	20	120	166,67	1,01	0,16	5,40

Table B. Results of Analysis of Variance (ANOVA)

Source	DF	Adj SS	Adj MS	F-Value	P-Value
Model	28	302,488	10,8031	9,91	0,000
Blocks	2	0,019	0,0094	0,01	0,991
Linear	6	208,633	34,7721	31,91	0,000
Laser power [W]	2	135,407	67,7033	62,12	0,000
Point distance [μm]	2	50,984	25,4918	23,39	0,000
Time exposure [μm]	2	22,243	11,1213	10,20	0,000
2-Way Interactions	12	76,282	6,3568	5,83	0,000
Laser power [W]*Point distance [μm]	4	43,738	10,9346	10,03	0,000
Laser power [W]*Time exposure [μm]	4	14,280	3,5700	3,28	0,018
Point distance [μm]*Time exposure [μm]	4	18,263	4,5658	4,19	0,005
3-Way Interactions	8	17,555	2,1943	2,01	0,063
Laser power [W]*Point distance [μm]*Time exposure [μm]	8	17,555	2,1943	2,01	0,063
Error	52	56,673	1,0899		
Total	80	359,161			

where, R^2=84,22%